Supporting information

High Performance Organic Lithium Salt-Doped OFET with Optical Radical Effect for Photoelectric Pulse Synaptic Simulation and Neuromorphic Memory Learning

Yujiao Li, Gang He,* Wenhao Wang, Can Fu, Shanshan Jiang, Elvira Fortunato, Rodrigo Martins

Y. J. Li, G. He, W. H. Wang, C. Fu,
Field Effect Device & Flexible Display Lab, School of Materials Science and Engineering, Anhui University, Hefei 230601, P.R. China
E-mail: hegang@ahu.edu.cn
S. S. Jiang
School of Integrated Circuits, Anhui University, Hefei 230601, P.R. China
E. Fortunato, R. Martins
Department of Materials Science/CENIMAT-I3N, Faculty of Sciences and Technology, New University of Lisbon and CEMOP-UNINOVA Campus de Caparica 2829-516 Caparica, Portugal

Experimental Section:

Precursor Preparation: The dielectric material polyvinyl alcohol (PVA, Mw = 67 kDa) was purchased from Macklin. The Bis(trifluoromethane)sulfonimide lithium salt (Li-TFSI, 99%) and photoinitiator 2,2′-Bis(2-chlorophenyl)−4,4′,5,5′-tetraphenyl-1,2′-biimidazole (Cl-HABI) were purchased from Aladdin. The p-type highly π-extended organic D-A copolymer poly[2,5-bis(alkyl)pyrrolo[3,4-c]pyrrole-1,4(2H,5H)-dione-alt-5,5′-di(thiophene-2-yl)-2,2′-(E)-2-(2-(thiophene-2-yl)-vinyl)thiophene] (PDVT-10) with a concentration of 5 mg/mL was purchased from Derthon Optoelectronic Materials Science Technology Co Ltd. All materials utilized as received, without further purification. The PDVT-10 (5 mg) and the Cl-HABI (1.5 mg) were dissolved in 1 mL chloroform and stirred for 3 h at 50 ℃ to obtain a uniform solution. The PVA (0.5 g) was dissolved in 9.5 ml deionized water by stirring the mixture at 80 ℃ for 6 h and then left to stand for 8 h at room temperature. To obtain Li-TFSI doped PVA precursor solutions, 0.5 g of PVA and different quality of Li-TFSI (0.1g, 0.2 g, 0.3g) were weighed and dissolved in different volumes of deionized water (9.4 ml, 9.3 ml, 9.2ml) as solvent, respectively.

Devices Fabrication: The purchased commercially available heavily doped silicon wafer was used as the gate. The silicon wafers were sequentially cleaned by ultrasonication with ethanol, 70 ℃ mixed solution and deionized water for 10 min, where the mixed solution was prepared with deionized water, ammonia and hydrogen peroxide in a volume ratio of 7:2:1. Finally, the wafers were purged and dried with nitrogen. The PVA solution was spin-coated on the silicon wafers at 1000 rpm in 50 s

and annealed at 50 °C for 1 h as a dielectric layer. After the semiconductor solution was mixed in a certain proportion, the mixed solution was spin-coated on the dielectric layer at 1000 rpm for 60 s and annealed at 150 °C for 10 min to form an active layer. Finally, 50 nm gold was thermally evaporated onto the active layer through the shadow mask as the source/drain electrode.

Films Characterization: The morphology and roughness degree of organic thin films were observed using AFM (HITACHI Japan). The optical absorption properties of organic thin films were examined by UV-vis spectroscopy (UV-2550, Shimadzu). The UPS (Thermo ESCALAB 250XI) was employed to analyze the valence band top and secondary electron cutoff edge, which could obtain the energy band structure and work function information of the films. The capacitance of dielectric films were investigated by the impedance analyzer (Keysight, E4990A).

Devices Characterization: The electrical characteristics of the transistors were measured by the semiconductor parameter analyzer B1500A (Agilent), 4200SCS (Keithley) and FS-Pro (PDA). The UV light source for the experiments was provided by light driver (DC2200, Thorlabs).

Supplementary Figures：

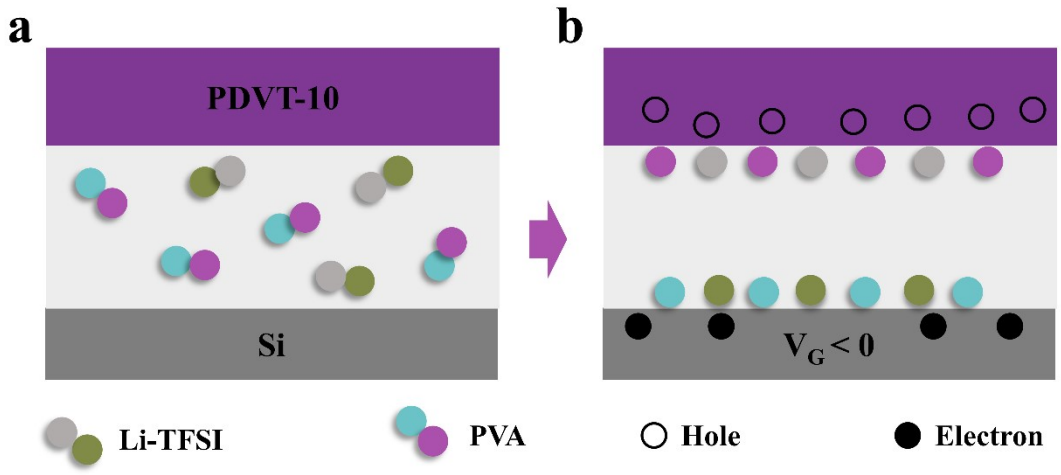

Fig. S1 Working Mechanism of PVA Gate dielectric layer doped with Organic Lithium Salts. (a) before applying negative voltage and (b) after applying voltage.

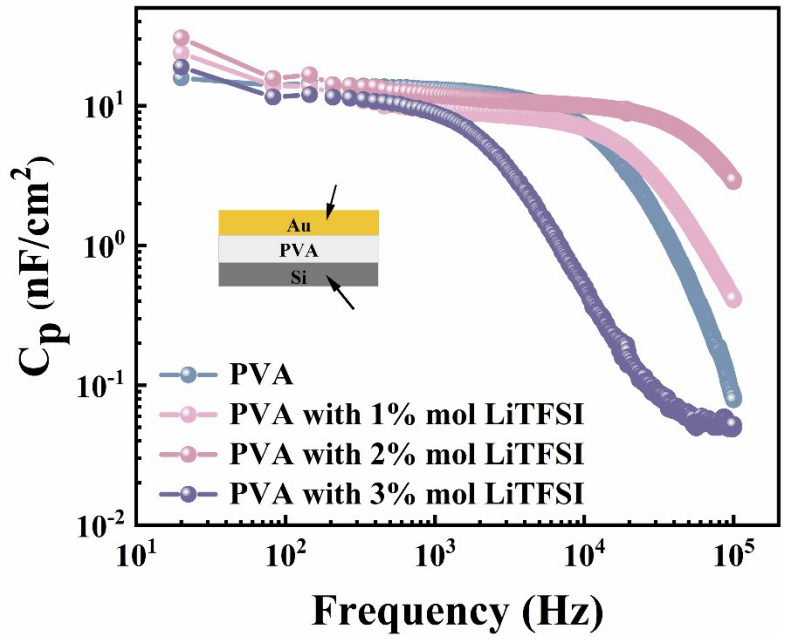

Fig. S2 Variation of capacitance per unit area with frequency of devices doped with different concentrations of Li-TFSI.

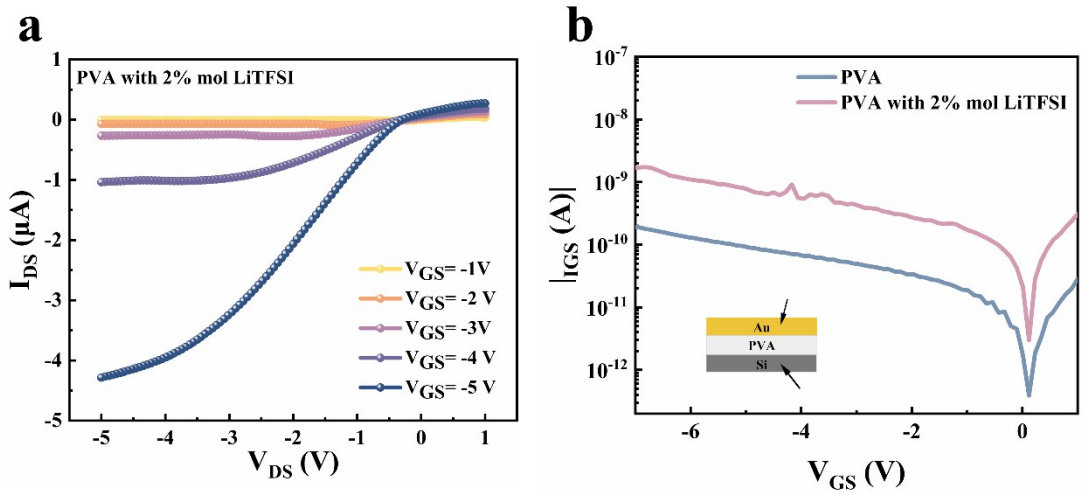

Fig. S3 (a) Output characteristic Curve of PVA device doped with 2% mol Li-TFSI. (b) Leakage current curves of PVA and PVA-TFSI gate dielectric devices.

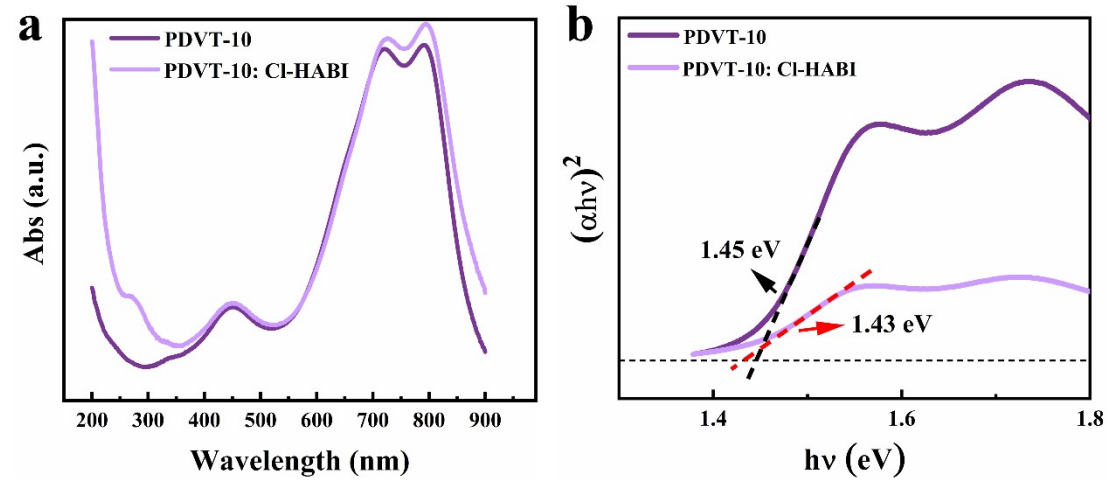

Fig. S4 (a) Ultraviolet absorption Spectra and (b) Bandgap diagrams of PDVT-10 organic thin films before and after the introduction of Cl-HABI.

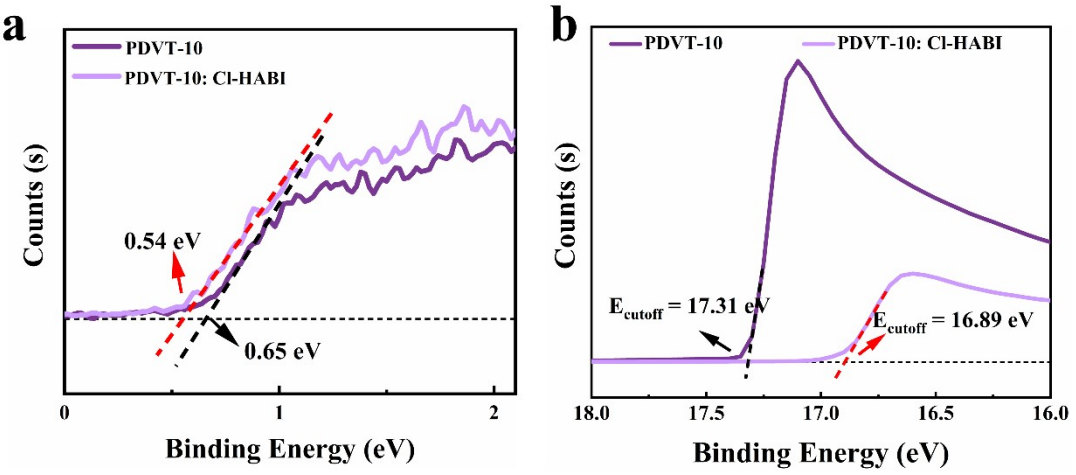

Fig. S5 (a) Valence band top and (b) secondary electron cutoff edge of PDVT-10 and PDVT-10/Cl-HABI thin films measured by UPS.

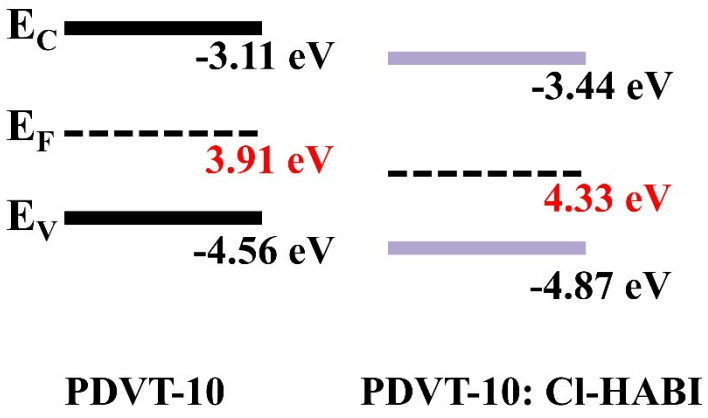

Fig. S6 Band structure diagrams of PDVT-10 and PDVT-10/Cl-HABI thin films.

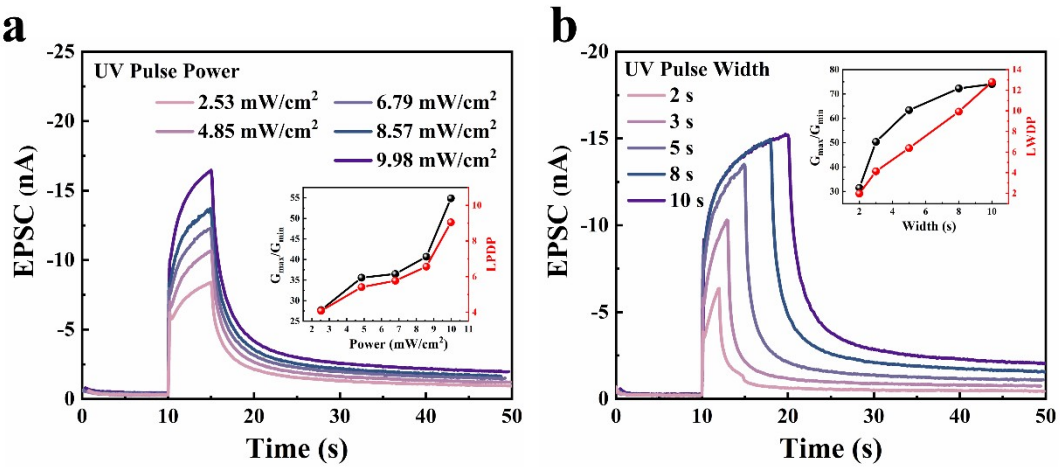

Fig. S7 Long-term/short-term potentiation transition and synaptic weights modulated based on PVA dielectric device by Ultraviolet light stimulus with corresponding (a) power and (b) width.

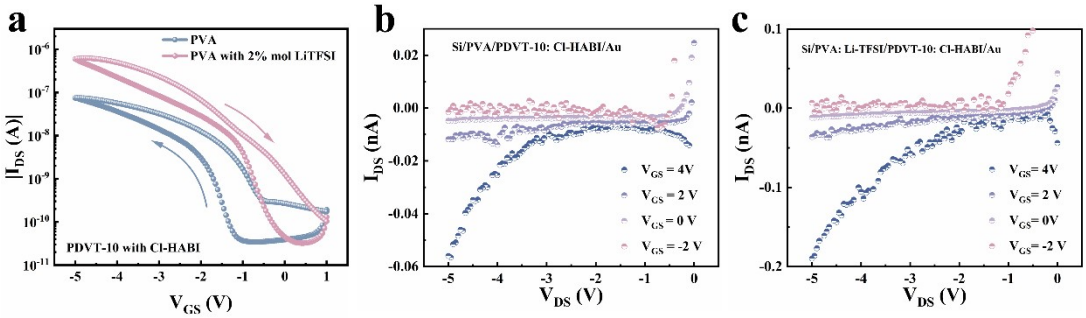

Fig. S8 (a) Transfer characteristic curve of PDVT-10/Cl-HABI devices before and after Li-TFSI doping with PVA. The Output characteristic curve for PDVT-10/Cl-HABI devices (b) before and (c) after doping with Li-TFSI in PVA.

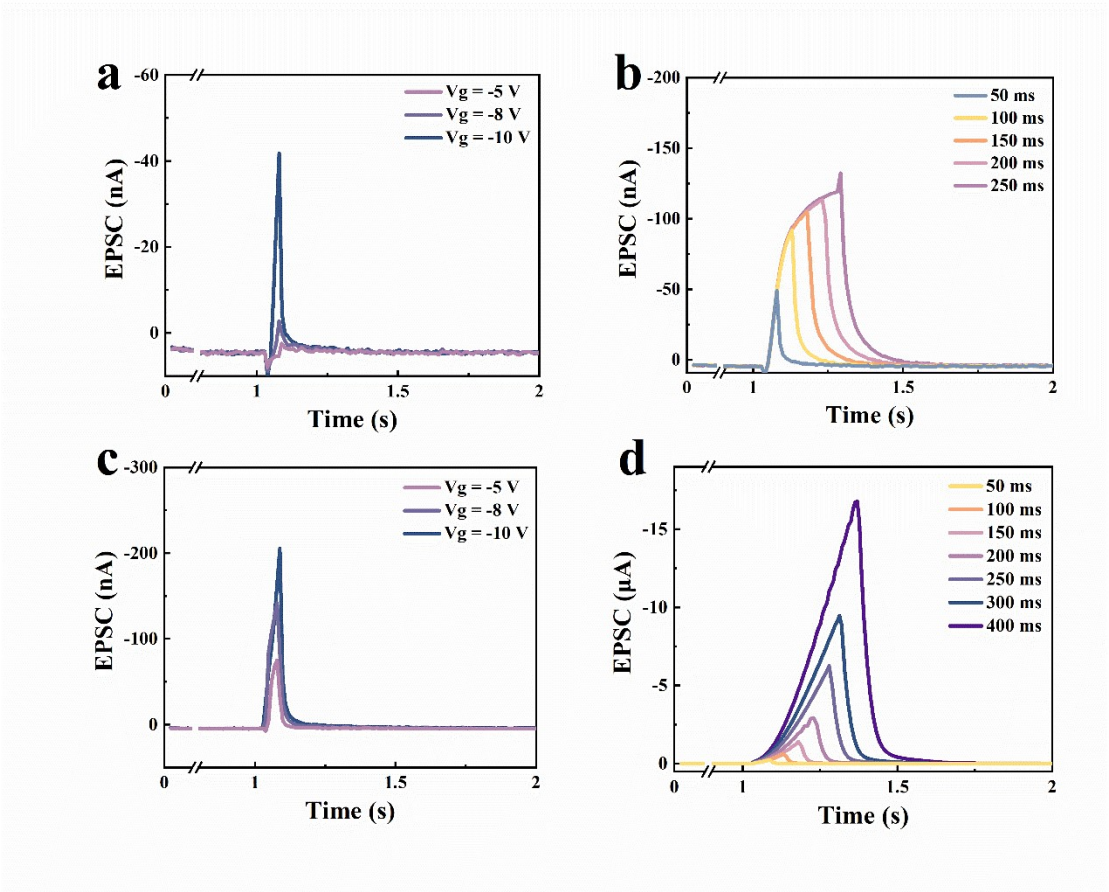

Fig. S9 The EPSC behaviors triggered by gate stimulus of various (a) intensities, and (b) durations of PDVT-10/Cl-HABI devices based on PVA gate dielectric. The EPSC behaviors triggered by gate stimulus of various (c) intensities, and (d) durations of PDVT-10/Cl-HABI devices based on PVA: Li-TFSI.

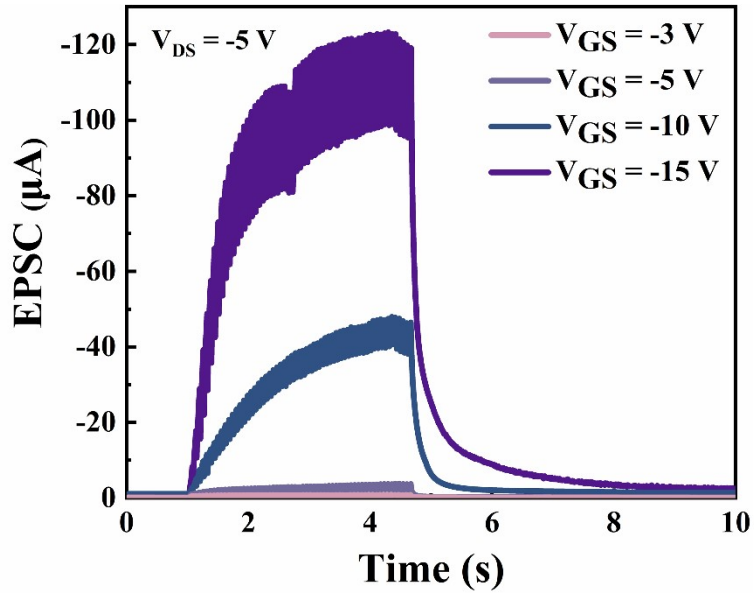

Fig. S10 The EPSC behaviors triggered by different pulse amplitudes of PDVT-10/Cl-HABI devices based on PVA: Li-TFSI.

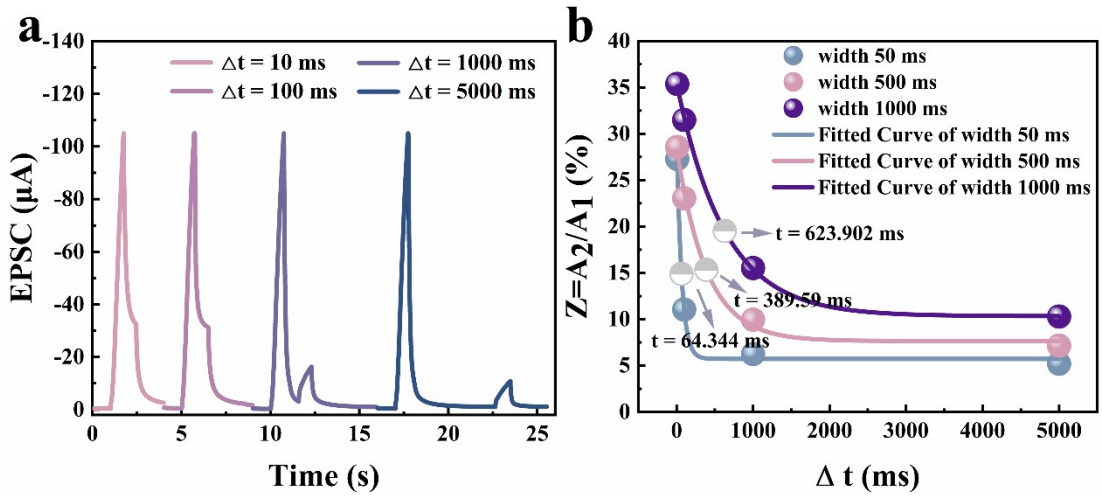

Fig. S11 (a) The EPSC of PDVT-10/Cl-HABI devices based on PVA: Li-TFSI with pulse width of 1000ms at different time intervals. (b) The Z index plotted as a function of the time interval between two continuous stimuli (Δt) with different pulse widths of the device.

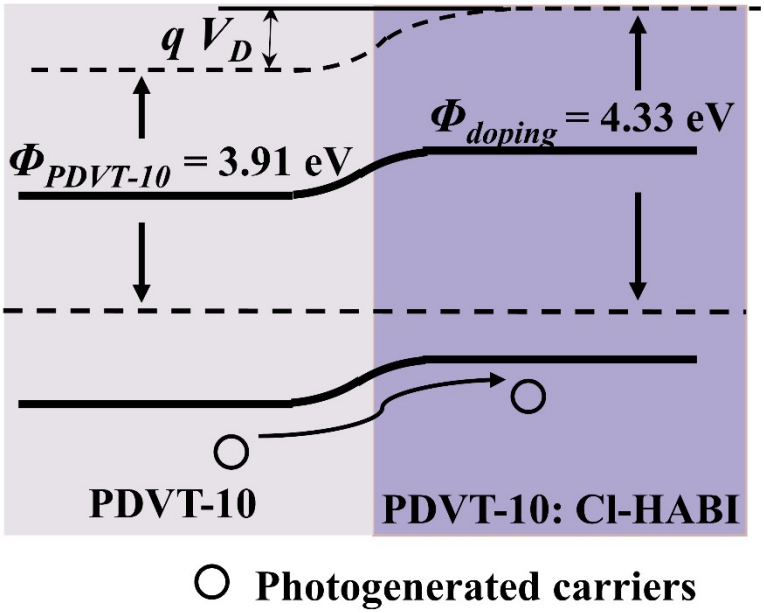

Fig. S12 Band structure of PDVT-10 and PDVT-10: Cl-HABI heterojunctions.

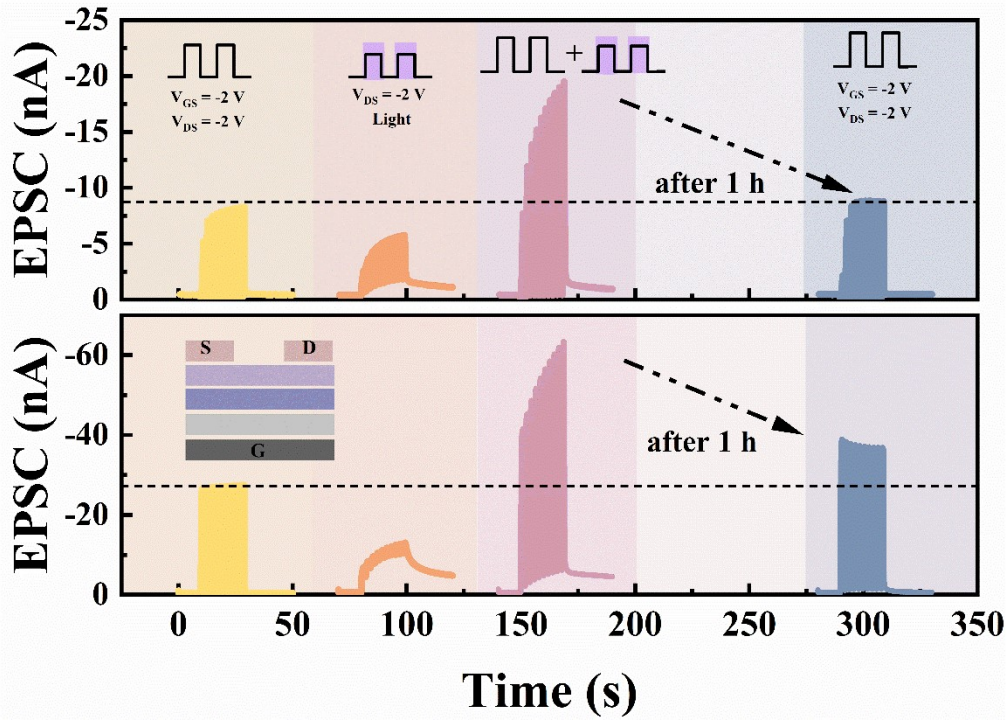

Fig. S13 Comparison of photoelectric synergistic effect between single-channel and double-channel layer artificial synaptic device.

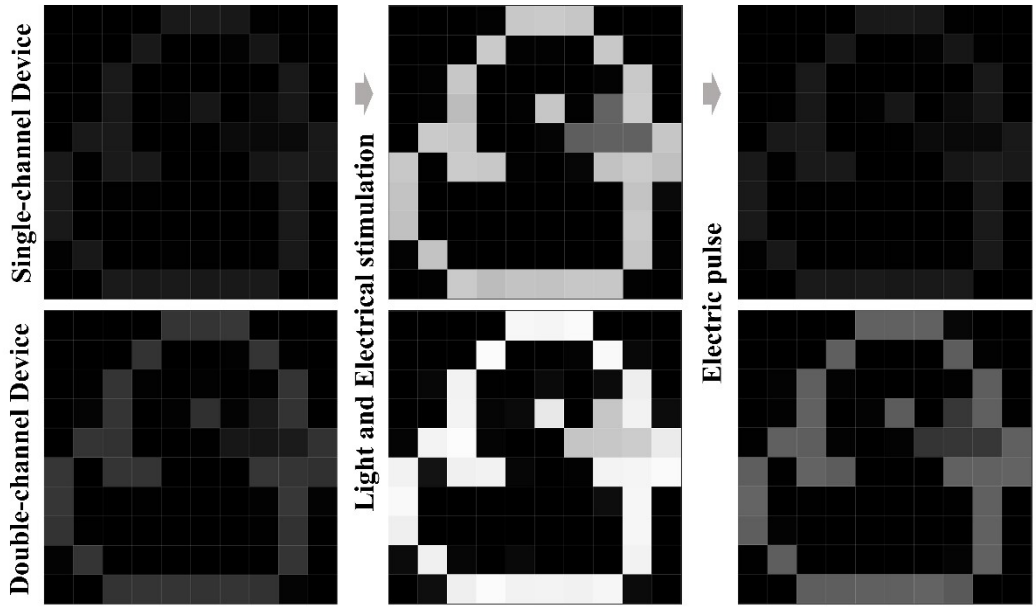

Fig. S14 The photoelectric synergism is associated with the grayscale pixel image, and the "duckling" image refresh process is displayed on the 10 × 10 synaptic unit, which simulates the image grayscale change caused by the volatile behavior of the device, by the memory behavior of single-channel and double-channel devices.

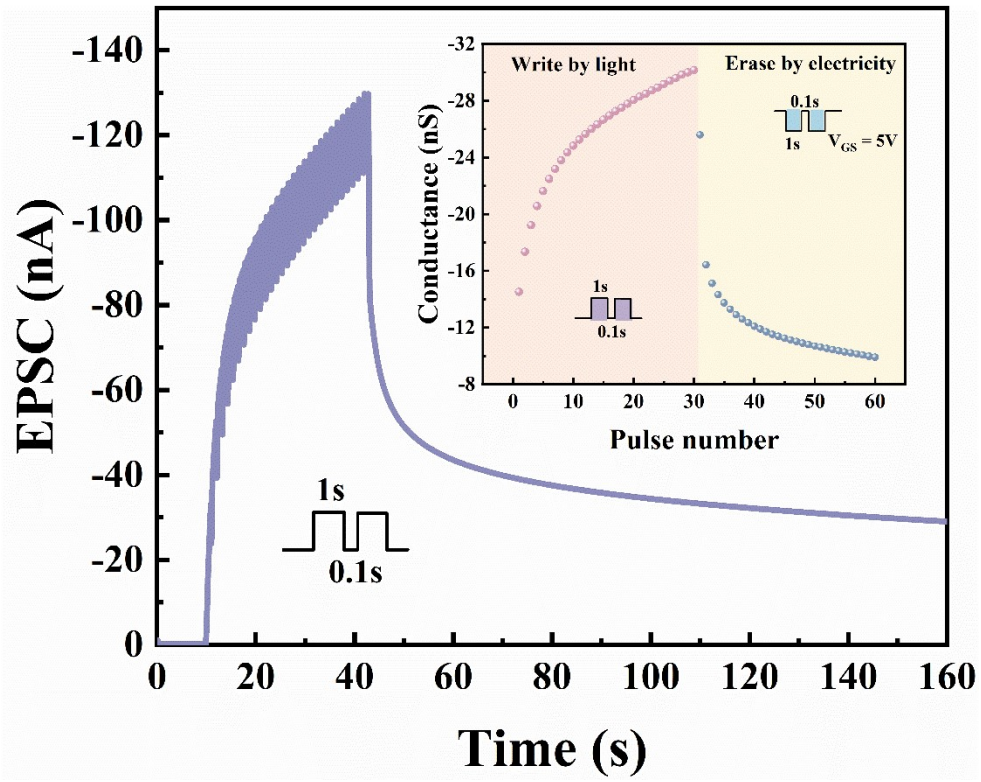

Fig. S15 Long-term characteristics optical pulse induction based double-channel layer artificial synaptic device and conductance changes in the process of optical writing and electrical erase with 30 consecutive light pulses and positive voltage pulses (V_{GS}, Pulse = 5 V, V_{DS} = -5 V, pulse width = 1 s, interval = 0.1 s).

Table S1. Comparison of optoelectronic performance of OFETs with PDVT-10 as channel layer.

device stack	Electric pulse synaptic simulation	Optical pulse synaptic simulation	Ref
Si/SiO_2/PVP+QDs /PDVT-10/Au		✧ Light-induced multi-gate synaptic devices realize logic circuits and classical conditioning experiment.	[1]
Si/SiO_2/DAE/ PDVT-10/Au		✧ Construction of neural network based on multimode conversion of DAE molecules under UV-vis light. (Pattern recognition)	[2]
Si/SiO_2/PDVT-10: $CsPbBr_3$ QDs/Au		✧ Photo-induced synaptic properties and digital recognition applications by quantum dot blending	[3]
Si/SiO_2/PDVT-10: N2200/Au	✧ Realization of 58V memory window and electrical pulse stimulation with bulk heterojunction and vertical structure. (STP, LTP)		[4]
Si/PVA: Malic acid/PDVT-10/Au	✧ bi-mode electrolyte-gated synaptic transistor with additional acid doping to regulate the sensitivity of artificial nociceptors. (Pressure-mapping circuits.)		[5]
Si/SiO_2/P(VDF-TrFE)/Al_2O_3/Ag NWs/PDVT-10: PCBM/Ag		✧ Ferroelectric-polarized photodetector with vertical structure (image sensing application)	[6]

Si/SiO_2/MXene: TiO_2/PDVT-10/Au		✧ optical synaptic properties, learning-forgetting-relearning, attention regulation signals, Dynamic target detection	[7]
Si/PVA: Li-TFSI/PDVT-10: Cl-HABI/Au	✧ PVA: Li-TFSI promotes EDL-effect, electric pulse analog high-pass filtering, (Image sharpening, Pain sensitization)	✧ Cl-HABI optical radical effect, light pulse LTP, (Photoelectric synergism, Image refresh, Learning and forgetting process)	This work

REFRENCES

1. W. He, Y. Fang, H. Yang, X. Wu, L. He, H. Chen and T. Guo, *J. Mater. Chem. C*, 2019, **7**, 12523-12531.
2. E. Li, W. He, R. Yu, L. He, X. Wu, Q. Chen, Y. Liu, H. Chen and T. Guo, *ACS Appl. Mater. Interfaces*, 2021, **13**, 28564-28573.
3. C. Wang, Q. Sun, G. Peng, Y. Yan, X. Yu, E. Li, R. Yu, C. Gao, X. Zhang, S. Duan, H. Chen, J. Wu and W. Hu, *Sci. China-Mater.*, 2022, **65**, 3077-3086.
4. C. Gao, H. Yang, E. Li, Y. Yan, L. He, H. Chen, Z. Lin and T. Guo, *ACS Photonics*, 2021, **8**, 3094-3103.
5. R. Yu, Y. Yan, E. Li, X. Wu, X. Zhang, J. Chen, Y. Hu, H. Chen and T. Guo, *Mater. Horizons*, 2021, **8**, 2797-2807.
6. Q. Chen, D. Lai, L. He, y. Yujie, E. Li, Y. Liu, H. Zeng, H. Chen and T. Guo, *ACS Appl. Mater. Interfaces*, 2021, **13**, 1035-1042.
7. N. Qin, Z. Ren, Y. Fan, C. Qin, C. Liu, W. Peng, B. Huang, H. Chen and T. Guo, *J. Mater. Chem. C*, 2024, DOI: 10.1039/D4TC00473F.